Variations in diurnal and seasonal net ecosystem carbon dioxide exchange in a semiarid sandy grassland ecosystem in China's Horqin Sandy Land

Yayi Niu[a,b,c,e], Yuqiang Li[a,b,c,*], Hanbo Yun[a,d,e], Xuyang Wang[a,b,c], Xiangwen Gong[a,b], Yulong Duan[a,b,c], Jing Liu[a]

[a] Northwest Institute of Eco-Environment and Resources, Chinese Academy of Sciences, Lanzhou 730000, China

[b] University of Chinese Academy of Sciences, Beijing 100049, China

[c] Naiman Desertification Research Station, Northwest Institute of Eco-Environment and Resources, Chinese Academy of Sciences, Tongliao 028300, China

[d] State Key Laboratory of Frozen Soil Engineering, Northwest Institute of Eco-Environment and Resources, Chinese Academy of Sciences, Lanzhou, Gansu 730000, China

[e] Center for Permafrost (CENPERM), Department of Geosciences and Natural Resource Management, University of Copenhagen, DK-1350 Copenhagen, Denmark

* *Correspondence to*: Yuqiang Li (liyq@lzb.ac.cn)

Abstract

Grasslands are major terrestrial ecosystems in arid and semiarid regions, and play important roles in the regional carbon dioxide (CO_2) balance and cycles. Sandy grasslands are sensitive to climate change, yet the magnitudes, patterns, and environmental controls of their CO_2 flows are poorly understood. Here, we report the results from continuous year-round CO_2 flux measurements in 5 years from a sandy grassland in China's Horqin Sandy Land. The grassland was a net CO_2 source at an annual scale, with a mean annual net ecosystem CO_2 exchange (NEE) of 49 ± 8 g C m^{-2} yr^{-1} in the years for which a complete dataset was available (2015, 2016, and 2018); Annual precipitation had the strongest effect on annual NEE. The grassland's carbon sequestration increased with increasing precipitation. In the spring, NEE increased with increasing soil temperature (T_{soil}) and increasing precipitation. In the summer, NEE was dominated by the frequency and amount of effective precipitation events. In the autumn, NEE increased with increasing T_{soil} and near-surface soil water content (SWC), but decreased with increased SWC deeper in the soil. In the winter, NEE decreased with increasing T_{soil} and SWC. The sandy grassland was a net annual CO_2 source at an annual scale. On the one hand, this is because drought decreased carbon sequestration by the annual plants. On the other hand, the study site is recovering from degradation, so vegetation productivity is still low. Therefore, the ecosystem has not yet transitioned to a CO_2 sink and long-term observations will be necessary to reveal the true source or sink intensity and its response to environmental and biological factors.

Keywords: Net ecosystem CO_2 exchange (NEE); Gross primary productivity (GPP); ecosystem respiration (R_{ec}); Eddy covariance; Horqin Sandy Land

1 Introduction

Arid and semiarid ecosystems cover 30 to 40 % of the global terrestrial surface (Poulter et al., 2014). The extent and distribution of these areas are increasing in response to factors such as climate change, changes in wildfire frequency and intensity, and changes in land use (Asner et al., 2003; Hastings et al., 2010). These ecosystems are important because they account for 30 to 35 % of terrestrial net primary productivity

(Gao et al., 2012; Liu et al., 2016a) and approximately 15 % of the global soil organic carbon pool (Lal, 2004; Liu et al., 2016a). Thus, these areas are important contributors to the global carbon budget due to their wide distribution (Emmerich, 2003; Nosetto et al., 2006; Poulter et al., 2014; Zhou et al., 2020), and arid and semiarid ecosystems will have significant effects on the global carbon cycle and carbon balance (Lal, 2004; Biederman et al., 2017). However, the availability of continuous, long-term measurements of water and net ecosystem CO_2 exchange (NEE) has lagged in arid and semiarid ecosystems (Baldocchi et al., 2001; Hastings et al., 2010; Biederman et al., 2017). Recent research on the relationship between NEE and water in drylands has focused on the southwestern United States (Scott et al., 2015; Biederman et al., 2016, 2017) and Australia (Cleverly et al., 2016; Li et al., 2017). For instance, Biederman et al. (2016) showed that across a climatic and ecological gradient in semiarid North American ecosystems, photosynthesis showed a saturating spatial relationship to precipitation, and evapotranspiration was a better proxy for the water available to drive NEE after accounting for hydrologic losses. Both photosynthesis and respiration showed similar site-level sensitivity to interannual changes in evapotranspiration among the studied ecosystems. Compared with the more constant sink that is typically measured in mesic ecosystems, dryland ecosystems showed a wide range of carbon sink or source functions for diverse vegetation types (Biederman et al., 2017). However, to our knowledge, there has been no report on the intra-annual and interannual variation of ecosystem-scale NEE and its components in China's Horqin Sandy Land, an important dryland ecosystem in northern China.

Desertification occurs in more than two-thirds of the area of arid and semiarid ecosystems (Lal, 2001). This may cause a serious imbalance in the structure and function of these ecosystems (Huenneke et al., 2002; Vest et al., 2011), especially in terms of whether the ecosystem functions as a carbon source or sink (Shachak et al., 1998; Gang et al., 2011). Grazing exclusion is a common method used to combat desertification in the world's arid and semiarid areas (Mureithi et al., 2010; Sousa et al., 2012). For example, Sun et al. (2015) suggested that proper exclosures promoted the

recovery of degraded sandy grassland and more sustainable use of sandy grassland resources.

The Horqin Sandy Land is the largest sandy land in China, and nearly 80 % of the area has been desertified (Li et al., 2019). Here, we define "sandy land" as land covered by a sandy soil, with a vegetation cover less than 5%, which includes areas of sandy desert (Yan et al., 2003). Sandy land includes multiple overlapping ecotones, including transition zones between areas with different population pressures, between semi-humid and semiarid areas, and in typical agro-pastoral ecotones. The ecological environment is fragile and extremely sensitive to climate change and human activities (Bagan et al., 2010; Zhao et al., 2015). The region's sandy grassland grows on aeolian sandy soils or areas with sandy soils as the substrate, and is typical of the grassland vegetation that develops in sandy land (Munkhdalai et al., 2007). This grassland ecosystem is widespread in the Horqin Sandy Land (Zhao et al., 2007).

Research showed that the restoration of degraded sandy grassland can increase its productivity and carbon sequestration, and that the ecosystem can begin to act as a carbon sink (Ruiz-Jaen and Aide, 2005; Zhao et al., 2016). However, other studies showed that it was a carbon source (Li et al., 2012; Niu et al., 2018). There have been relatively few long-term studies of sandy grassland at the ecosystem level, so we do not yet fully understand the characteristic of NEE and its components, gross primary productivity (GPP) and ecosystem respiration (R_{ec}), at an ecosystem scale, particularly for sandy grassland protected by grazing exclosures, and more data are needed, particularly for semiarid sandy land (Barrett, 1968; Czobel et al., 2012).

Precipitation is one of the factors that most strongly affects NEE in arid and semiarid areas (Scott et al. 2015; Biederman et al. 2016). Slight changes to the amount and frequency of precipitation may trigger complex interactions among biochemical processes at the ecosystem level (Emmerich and Verdugo, 2008; Cleverly et al., 2016). Small precipitation amounts can improve the near-surface (<10 cm) soil water content (SWC) and stimulate ecosystem carbon emission, mainly by promoting microbial respiration, in arid and semiarid areas (Schwinning and Sala, 2004). Larger

104 precipitation amounts can increase SWC in deeper levels of the soil and trigger
105 sequestration processes (Hao et al., 2010). To better understand the effects of
106 precipitation on NEE, we asked the following question: Is there a threshold of "effective
107 precipitation" that determines whether ecosystem carbon fluxes will lead to net
108 sequestration or net emission in sandy grasslands?

109 Precipitation is characterized by discrete events in arid and semiarid regions, with
110 high variability in the amount, duration, and frequency of precipitation at intra-annual
111 (e.g., seasonal) and inter-annual scales (Hao et al., 2010; Ponce Campos et al., 2013).
112 These discrete and largely unpredictable events may lead to pulsed availability of soil
113 water and nutrients, with both spatial and temporal variation (Zhao and Liu, 2011). The
114 response of photosynthesis and respiration to precipitation is seasonally specific
115 because of differences in the depth of soil water infiltration and because these processes
116 differ in their sensitivity to temperature (Li and Zhou, 2012). Spring and autumn
117 precipitation are important controls on the beginning and end dates of the growing
118 season, so the ability of these events to change carbon accumulation or emission should
119 not be ignored, especially in semiarid and arid regions (Prevéy et al., 2014; Shen et al.,
120 2015). This is particularly true when relatively low temperatures limit soil microbial
121 respiration during certain periods (Knorr et al., 2005). Summer precipitation is thought
122 to primarily influence shallow soil moisture, thereby stimulating the activity of
123 shallowly rooted plants, whereas a combination of high temperatures and high soil
124 moisture stimulate the respiratory response by soil microbes (Sponseller, 2006). The
125 amount and frequency of summer precipitation may therefore play an important role in
126 regulating inter-annual variations of the ecosystem carbon balance (Scott et al., 2009;
127 Wu et al., 2012). Moreover, we found no reports on the response of ecosystem-scale
128 NEE and its components to seasonal and annual precipitation, and the response
129 mechanisms are uncertain for the sandy grassland in the Horqin region. Therefore, long-
130 term data are required to fully understand how changes in seasonal and annual
131 precipitation influence NEE, GPP, and R_{ec} in grassland ecosystems such as those in the
132 Horqin Sandy Land. Understanding the consequences of climate change that are

associated with changes in precipitation patterns, and that affect soil water regimes, may be critical for developing strategies to preserve or restore these sandy grasslands.

In this paper, we present the results from continuous (14 September 2014 to 31 December 2018) *in situ* monitoring of CO_2 dynamics in the Horqin Sandy Land's sandy grassland using the eddy covariance technique, and quantify the temporal variation of NEE and the factors that control it. We had the following goals: (1) To quantify the annual, seasonal, and diurnal variation in NEE, GPP, and R_{ec}. We hypothesized that the sandy grassland is a carbon source at the ecosystem scale, because the sandy grassland is dominated by annual plants that are vulnerable to drought (Li et al., 2016; Kang et al., 2018), and because the ecosystem is recovering from degradation, leading to low vegetation productivity (Sun et al., 2015). (2) To explore the effects of changes in precipitation amount and frequency on seasonal and annual NEE, GPP, and R_{ec}. Based on the response thresholds of shrubs and herbs to precipitation in arid and semiarid areas (Hao et al., 2010; Zhou et al., 2020), we hypothesized that an "effective precipitation" threshold would exist at around 5 mm, which could alter soil moisture in deeper layer and affect carbon fluxes in the sandy grassland ecosystem. We also hypothesized that spring, summer, and autumn precipitation would have different impacts on the ecosystem CO_2 exchange through differential effects on plant photosynthesis and soil microbial respiration (Scott et al., 2009).

2 Materials and methods

2.1 Experimental site

Our study was conducted in a sandy grassland in the southern part of the Horqin Sandy Land, Inner Mongolia, China, at the Naiman Desertification Research Station of the Chinese Academy of Sciences (42 °55′ N, 120 °42′ E) (Fig. 1). The terrain is flat, and it evolved from reclamation of sandy grassland for agriculture to severe desertification, after which cultivation was abandoned and grazing exclosures were established to allow natural recovery of the vegetation, starting in 1985 (Zhao et al., 2007). Thus, the grassland had been recovering naturally for nearly 30 years when our study began. At an elevation of 377 m a.s.l., the study area has a continental semiarid

monsoon temperate climate regime. The mean annual temperature is 6.8 ℃, with mean monthly temperatures ranging from -9.63 ℃ in January to 24.58 ℃ in July. Average annual precipitation is approximately 360 mm, with 70 % of the precipitation occurring during the growing season, between June and August. Annual mean potential evaporation is approximately 1973 mm. The annual frost-free period is 130 to 150 days. The most common soil type in the study region is a sandy chestnut soil, but most of the soil has been degraded by a combination of climate change and anthropogenic activity (unsustainable grazing or agriculture) into an aeolian sandy soil under the action of wind erosion (Zhao et al., 2007), with coarse sand, fine sand, and clay-silt contents of 92.7, 3.3, and 4.0 % in the topsoil to a depth of 20 cm. The contents of soil organic carbon and total nitrogen were 1.27 and 0.21 g kg^{-1}, respectively. Vegetation cover in the study area ranged from 50 to 70 %. The dominant plant species were annual herbs, including *Artemisia scoparia*, *Setaria viridis*, *Salsola collina*, and *Corispermum hyssopifolium* (Niu et al., 2018).

2.2 Eddy covariance observations

An eddy covariance flux tower (2.0 m high) was installed at the center of the observation field (Fig. 1b, c). We have continuously monitored CO_2, water, and heat fluxes at the tower using the eddy covariance system since late 2014. The site was flat and comprised homogeneous vegetation. The upwind fetch was about 200 m under unstable atmospheric conditions, which was greater than the flux footprint (Schmid, 1997; Xu and Baldocchi, 2004). The eddy covariance system consisted of an LI-7500 infrared gas analyzer (Li-Cor Inc., Lincoln, NE, USA), with a precision of 0.01 μmol m^{-2} s^{-1} and an accuracy within 1 % of the reading for measurements at 30-min mean intervals, and a CSAT-3 three-dimensional ultrasonic anemometer (Campbell Scientific, Inc., Logan, UT, USA), with a precision of 0.1 ℃ and an accuracy of 1 % for the readings at 30-min mean intervals. Raw 10-Hz data were recorded by a CR3000 datalogger (Campbell Scientific, Logan, UT, USA). The operation, calibration, and maintenance of the eddy covariance system followed the manufacturers' standard procedures. The LI-7500 was calibrated every 6 months for CO_2, water vapor, and dew

point values using calibration gases and dew point generator measurements supported by the China Land–Atmosphere Coordinated Observation System (Yun et al., 2018). We cleaned the mirror of the LI-7500 every 15 days to maintain the automatic gain control value below its threshold (55 to 65). All of the instruments were powered by solar panels connected to a battery.

2.3 Micrometeorological measurements

Along with the flux measurements obtained by the eddy covariance equipment, we measured standard meteorological and soil parameters continuously with an array of sensors. A propeller anemometer was installed at the top of the meteorological tower to measure the wind speed and direction. Net solar radiation (R_n, W m^{-2}) was measured by a four-component radiometer (CNR-1, Kipp and Zonen, Delft, the Netherlands) installed at 1 m above the ground. The air temperature (T_{air}, °C) and relative humidity (%) instruments (HMP45C, Vaisala Inc., Helsinki, Finland) were mounted at 2 m above the ground to measure the T_{air}, relative humidity, and atmospheric pressure (kPa). Precipitation (mm) measurements were obtained from a meteorological station 400 m from the study site. Total daily precipitation was treated as a single event rather than a series of events. The daily events were separated into size classes for evaluation of the number of events per class and the effect on CO_2 fluxes (Emmerich and Verdugo, 2008).

We installed five CS109 temperature probes (Campbell Scientific) and five CS616 moisture probes (Campbell Scientific) in the soil at depths of 10, 20, 30, 40, and 50 cm to measure soil temperature (T_{soil}, °C) and soil water content (SWC, %). Two self-calibrating HFP01 soil heat flux (SHF, W m^{-2}) sensors (Hukseflux, Delft, the Netherlands) were buried 5 and 10 cm below the ground to obtain the SHF data. All of the environmental parameters were measured simultaneously with the eddy covariance measurements, and all data were recorded as 30-min mean values with a CR3000 datalogger.

2.4 Data quality and gap-filling method

We used the EddyPro 6.2.0 software (Li-Cor, Lincoln, NE, USA) to process the 10-Hz raw eddy covariance data. Processing included spike removal, lag correction,

secondary coordinate rotation, Webb–Pearman–Leuning correction, and sonic virtual temperature conversion (Webb et al., 1980). We used the data processing method of Lee et al. (2004) to process the 30-min mean raw flux measurements to ensure their quality. Processed data were further corrected for weather effects and sensor uncertainty using the following procedure: (1) We removed data gathered during precipitation events, power failures, and sensor maintenance or malfunction. (2) We excluded unrealistic CO_2 flux data (values outside the range of –2.0 to 2.0 mg CO_2 m^{-2} s^{-1}). (3) We rejected data collected during periods of insufficient turbulent mixing using a friction-velocity filter (u^*< 0.1 m s^{-1}) for data collected at night (Reichstein et al., 2005; Scott et al., 2009). Based on the R_n, NEE was classified as the daytime exchange (NEE_{day}; $R_n \geq 1$ W m^{-2}) or the night-time exchange (NEE_{night}; R_n < 1 W m^{-2}). This screening resulted in the rejection of 20 to 30 % of the flux data, depending on the period.

We used several strategies to compensate for missing data. We used linear interpolation to fill gaps that were shorter than 2 h. For longer gaps, we handled the gap in the NEE_{day} using the mean diurnal variation with a 7-day window (Falge et al., 2001), and handled the gap in the NEE_{night} using the following equation 1, the parameter values were calculated with a 7-day moving window using version 22 of the SPSS software (IBM, Armonk, NY, USA) (Lloyd and Taylor, 1994; Reichstein et al., 2005).

$$NEE_{night} = R_0 \exp(b \ T_{10}) \quad (1)$$

R_0 is the base ecosystem respiration rate when the soil temperature is 0 °C, b is an empirically determined coefficient, and T_{10} is the soil temperature at a depth of 10 cm. Daytime ecosystem respiration can be estimated by extrapolation from the parameterization derived from Eq. (1). We did not attempt to fill in gaps longer than 7 days, and treated those gaps as missing data. Gross primary productivity (GPP) was obtained as follows:

$$GPP = R_{ec} - NEE \quad (2)$$

We used the standard sign convention for NEE, with NEE > 0 indicating a net loss of CO_2 to the atmosphere (source) and NEE < 0 indicating net CO_2 uptake by the ecosystem (sink).

We evaluated the data quality based on the degree of energy closure (sensible heat + latent heat – net radiation – soil heat flux). The energy closure values for the sandy grassland from 2015 to 2018 were 86.5, 82.1, 57.7, and 85.2 %, respectively.

2.5 Statistical analyses

We performed correlation analysis (Pearson's r) and regression analysis using the SPSS software. Unless otherwise noted, we defined statistical significance at $p < 0.05$. Pearson's r was applied to confirm the strength of the relationships between parameters. Before regression analysis, we tested for collinearity (using a variance inflation factor of $0 < VIF < 10$) using the Kaiser–Meyer–Olkin (KMO) test and Bartlett's sphericity test. Collinearity was used to repartition the T_{soil} and SWC data. We considered KMO values > 0.50 and $p < 0.05$ for Bartlett's sphericity test to indicate acceptable data (Hair et al., 2005). The KMO value ranged from 0.52 to 0.78 and $p < 0.001$ for all Bartlett's sphericity test results for our data.

3 Results

3.1 Meteorological conditions

Figures S1 to S5 show the diurnal and seasonal variation of the meteorological factors during the observation period. The mean daily T_{air}, R_n, SHF at all depths, and T_{soil} at depths of 10, 20, 30, 40, and 50 cm showed unimodal seasonal variations in all 4 years. These parameters were therefore largely stable and did not differ greatly between years, except for the precipitation and SWC at all depths (Fig. S4b). Thus, precipitation and SWC were the main factors that influenced NEE, and we focused on them in our analysis. The annual precipitation totaled 212 mm in 2015, 277 mm in 2016, 313 mm in 2017, and 351 mm in 2018 (Fig. S4b). Yearly and seasonal variability in the total number of precipitation events and number of precipitation events within each size class was large, and the 0 to 5 mm size class was by far the dominant size class (Table 1). Zhao and Liu (2010) showed that precipitation less than 5 mm in arid and semiarid areas changes SWC primarily in the near-surface soil, and that precipitation events greater than 5 mm can effectively supplement root layer moisture at greater depths; it is therefore called "effective precipitation". Our result was consistent with this view

(Fig. 2). The essence of effective precipitation is that precipitation enters the soil below the surface layer, and becomes part of the soil water; that soil water is used either directly or indirectly by the vegetation, and has an impact on other ecological links (Joseph Turk et al., 2012). Therefore, we studied the influence of precipitation on NEE and its components in each season from the perspective of SWC. The climate was drier in 2015, 2016, and 2017 than in a normal year (based on the mean annual precipitation of 360 mm from 1960 to 2014), whereas 2018 was close to a normal year. The variation in soil water content was related to precipitation patterns. During the spring (March, April, and May), precipitation was relatively abundant, with mean precipitation of about 42 mm, which accounted for 12 to 20 % of the total annual precipitation. The majority of the precipitation (about 65 %) occurred in the summer (June, July, and August), with mean precipitation of about 197 mm. The autumn (September, October, and November) precipitation was similar to that in spring, with a mean precipitation of about 49 mm, which accounted for 14 to 23 % of the annual total. During the winter (December, January, and February), the mean precipitation of 0.6 mm accounted for only 1 to 6 % of the annual total, and was largely stable, with small differences among the years.

3.2 Annual, seasonal, and diurnal variability of NEE, GPP and R_{ec}.

We also observed clear seasonal variations in daily mean NEE, GPP, and R_{ec} from 2014 to 2018 (Fig. 3). Our results suggests that the sandy grassland was a net CO_2 source, with an annual mean NEE, GPP, and R_{ec} of 49 ± 8, 303 ± 29, and 352 ± 21 g C m^{-2} yr^{-1}, respectively, in the years for which a complete dataset was available (2015, 2016, and 2018) (Fig. 3f). (We omitted 2017 from this calculation because of large gaps in the data, described below.) NEE ranged from 35 g C m^{-2} yr^{-1} in 2018 to 63 g C m^{-2} yr^{-1} in 2015, whereas GPP ranged from 256 g C m^{-2} yr^{-1} in 2015 to 356 g C m^{-2} yr^{-1} in 2018 and R_{ec} ranged from 319 g C m^{-2} yr^{-1} in 2015 to 391 g C m^{-2} yr^{-1} in 2018. From 15 September to 23 December 2014, we measured a cumulative carbon release of 47 g C m^{-2}, with cumulative GPP and R_{ec} of 25 and 72 g C m^{-2}, respectively. From 15 February to 26 April 2017 and from 14 October to 6 November 2017, approximately 3

months of data were missing due to instrument maintenance and calibration, and the cumulative NEE, GPP, and R_{ec} were 64, 274, and 338 g C m^{-2}, respectively, for the remaining 9 months of the year. Note that the periods covered by the data are therefore not identical.

Figures 4 and 5 show the seasonal NEE, GPP, and R_{ec} and their diurnal cycles, respectively. In the spring, the sandy grassland was an atmospheric CO_2 source in all years, with NEE, GPP, and R_{ec} averaging 0.14 ±0.04, 0.60 ±0.06, and 0.74 ±0.02 g C m^{-2} d^{-1}, respectively (Fig. 4a). The diurnal NEE cycle was characterized by a single peak, and between 7:30 and 16:30, the ecosystem showed CO_2 absorption (Fig. 5a); the rest of the day was characterized by weak CO_2 emission. Note that although all times in China are reported as the Beijing time, the study site was not sufficiently far east of Beijing for this to affect the physiological meaning of these times. The average diurnal GPP was also characterized by a single peak from around 05:00 to around 19:30, and the diurnal R_{ec} was characterized by an approximately horizontal line at about 0.75 μmol m^{-2} s^{-1}.

In summer, the sandy grassland was a CO_2 sink in all years, with NEE, GPP, and R_{ec} averaging −0.66 ±0.08, 2.45 ±0.09, and 1.79 ±0.04 g C m^{-2} d^{-1}, respectively (Fig. 4b). The diurnal cycles of NEE and GPP were also characterized by a single peak, and the ecosystem CO_2 uptake reached its peak from around 10:30 to 12:00 (Fig. 5b). The diurnal R_{ec} pattern was similar to the spring, but at a higher level (about 1.79 μmol m^{-2} s^{-1}).

In autumn, the sandy grassland was a net source of atmospheric CO_2 in all years, with NEE, GPP, and R_{ec} averaging 0.50 ±0.03, 0.26 ±0.03, and 0.76 ±0.04 g C m^{-2} d^{-1}, respectively (Fig. 4c). The diurnal dynamics of NEE, GPP, and R_{ec} in autumn (Fig. 5c) were similar to those in spring (Fig. 5a), but the magnitudes of NEE and GPP in autumn were lower than in the spring. The diurnal R_{ec} was similar to the value in the spring, at about 0.73 μmol m^{-2} s^{-1}.

In winter, the grassland ecosystem functioned as a net CO_2 source in all years, with an average seasonal NEE of 0.59 ±0.02 g C m^{-2} d^{-1} (Fig. 4d). It should also be noted

that since the investigation started on 14 September 2014 and ended on 31 December 2018, the 2017 to 2018 winter was only about one-third of the usual length (i.e., it did not include data from January and February 2019). The diurnal dynamics of the winter NEE differed from the other seasons (Fig. 5d), with a minimum release value of 0.36 μmol m^{-2} s^{-1}, and with two emission peaks: at 0.78 μmol m^{-2} s^{-1} (08:00) and 0.85 μmol m^{-2} s^{-1} (16:30).

3.3 Response of NEE, GPP and R_{ec} to changes in environmental factors

At an annual scale, the major environment difference among the years with a complete dataset (2015, 2016, and 2018) was the amount of precipitation (Fig. S4). We analyzed the relationship between precipitation and the annual NEE, GPP, and R_{ec} in 2015, 2016, and 2018 (Fig. 6). We found that GPP and R_{ec} increased significantly with increasing annual precipitation, whereas NEE decreased significantly with increasing annual precipitation, indicating that the ecosystem's carbon sequestration capacity increased with increasing precipitation. Taken together, these results indicated different magnitudes and directions of response of the three parameters to annual precipitation.

At a monthly scale, the temperature, precipitation, and CO_2 fluxes (NEE, GPP, and R_{ec}) were relatively stable in winter (Fig. S4 and Fig. 4d). We have therefore focused on the relationships between NEE, its components, and the associated environmental factors in the other three seasons (Fig. 7-8). In the spring, the total monthly precipitation was significantly negatively correlated with NEE, but significantly positively correlated with GPP and R_{ec}, and GPP responded more strongly than R_{ec} to precipitation: $slope_{GPP}$ (0.88) > $slope_{Rec}$ (0.43). In summer, the total monthly precipitation was not significantly correlated with NEE, GPP, and R_{ec}. In autumn, the total monthly precipitation was significantly positively correlated with GPP and R_{ec}, with a similar strength of the response to precipitation: $slope_{Rec}$ (0.75) and $slope_{GPP}$ (0.72), therefore, NEE was not significantly correlated with total monthly precipitation.

At a daily scale, we calculated the correlations between the three CO_2 fluxes (NEE, R_{ec}, and GPP) and T_{soil} and performed regression analysis to understand their relationship with SWC at depths of 10, 20, 30, 40, and 50 cm in the spring, summer,

and autumn periods (Table S1, Fig. 8). In spring, NEE was significantly negatively correlated with T_{soil} from 0 to 50 cm, with SWC from 10 to 50 cm, and with SWC from 0 to 10 cm. GPP and R_{ec} were significantly positively correlated with these environmental factors. In summer, NEE was significantly negatively correlated with T_{soil} from 0 to 50 cm and with SWC from 40 to 50 cm, but was not significantly correlated with SWC from 0 to 10 cm. GPP and R_{ec} were significantly positively correlated with T_{soil} from 0 to 50 cm, SWC from 10 to 50 cm, and SWC from 0 to 10 cm. T_{soil} from 0 to 50 cm had a smaller impact on NEE, GPP, and R_{ec} in summer than in spring. In autumn, NEE was significantly positively correlated with T_{soil} from 0 to 50 cm and with SWC from 0 to 10 cm, but significantly negatively correlated with SWC from 10 to 30 cm. GPP and R_{ec} were significantly positively correlated with T_{soil} from 0 to 50 cm, SWC from 10 to 50 cm, and SWC from 0 to 10 cm.

4 Discussion

4.1 Annual and seasonal mean and diurnal variability

As we hypothesized, the sandy grassland ecosystem in the present study was a net CO_2 source at an annual scale, with an annual mean NEE of 49 ± 8 g C m^{-2} yr^{-1} in the years for which a complete dataset was available (2015, 2016, and 2018). This result was consistent with results for other ecosystems with similar climate and geographical conditions. For example, a grassland in New Mexico, United States, was a net source of 31 g C m^{-2} yr^{-1} during dry study periods (Petrie et al., 2015). A savanna in southern Arizona, United States, was also a net source of CO_2 to the atmosphere, with emission ranging from 14 to 95 g C m^{-2} yr^{-1} and the strength of the source increasing with decreasing precipitation (Scott et al., 2014). A woodland in central Australia was carbon-neutral during a dry year (Cleverly et al., 2013). In contrast, many other arid and semiarid dry ecosystems were a significant net sink for CO_2. For example, a desert ecosystem in the United States had net C sequestration of 102 to 110 g C m^{-2} yr^{-1} (Wohlfahrt et al., 2008); an artificial sand-binding vegetation system in China's Tengger Desert had net sequestration of 14 and 23 g C m^{-2} yr^{-1} (Gao et al., 2012); a phreatophyte-dominated desert ecosystem in China's Gurbantonggut Desert had net sequestration of

5 to 40 g C m^{-2} yr^{-1} (Liu et al., 2016a); and a shrubland in China's Mu Us desert had net sequestration of 77 g C m^{-2} yr^{-1} (Jia et al., 2014). There are several possible reasons for these differences among studies: (1) Our observations in 2015 and 2016 were in dry years with precipitation considerably below the long-term average, and because NEE was negatively related to precipitation (Fig. 6), this would have decreased carbon sequestration by the ecosystem. Previous studies showed that annual species such as the vegetation in our study area can be extremely vulnerable to drought (Jongen et al., 2011; Sun et al., 2015; Liu et al., 2016a). Drought was the main source of inter-annual variation in terrestrial carbon sequestration, as it decreases GPP and increases NEE (Webb et al., 1978; Sala et al., 1988; Ciais et al., 2005). (2) Our study site is still recovering from severe degradation, and has relatively low vegetation productivity, and the restoration of degraded sandy grassland ecosystems is a long process (Li et al., 2019). Therefore, the ecosystem has not yet reached the threshold at which it will change into a CO_2 sink, and it will be necessary to study NEE for a longer period to reveal when that change occurs and the ecosystem's long-term response to environmental and biological factors (Su et al., 2003; Niu et al., 2018).

In spring, the sandy grassland was a net CO_2 source in all years (Fig. 4a). Before the growing season, both GPP and R_{ec} increased with increasing temperature and precipitation (Niu et al., 2011; Rey et al., 2011). However, plants are just beginning to germinate in the spring, so the carbon sequestration capacity of the ecosystem is less than the carbon release capacity (Delpierre et al., 2010; Liu et al., 2016a; Zhang et al., 2016). Therefore, the ecosystem was a net CO_2 source.

In summer, the sandy grassland was a CO_2 sink in all years (Fig. 4b). Our results agree with previous results for the study area (Li et al., 2015), as well as with results for a semiarid savanna in Australia (Hutley et al., 2005) and a grassland in California (Ma et al., 2007). GPP and R_{ec} increased because of the favorable temperature and moisture conditions. However, because photosynthesis is greater than respiration during the peak of the growing season (Kemp, 1983; Liu et al., 2016a; Niu et al., 2018), the ecosystem became a net CO_2 sink.

In the autumn and winter, the sandy grassland was a net CO_2 source in all years (Fig. 4c, d). At the end of the growing season (in autumn), annual plants began to die and photosynthesis weakened (Fang et al., 2014). As a result, the ecosystem gradually transformed from a carbon sink to a carbon source (Keenan et al., 2009; Kiely et al., 2009). In winter, plants are either dead or dormant, so there is no C uptake.

At the diurnal scale, NEE in the spring and summer showed CO_2 uptake during the day (06:00-18:00), and CO_2 emission during the night (Fig. 5a, b). NEE decreased with increasing light intensity during the day, reached its peak value around noon, then increased until sunset, when the ecosystem changed from net carbon absorption to net carbon release (Wagle and Kakani, 2014; Jia et al., 2014).

In autumn and winter, the sandy grassland ecosystem showed CO_2 emission throughout the day (Fig. 5c, d). At a diurnal scale, the ecosystem showed carbon "uptake" in winter, but at a level too small to display in Figure 5d. This phenomenon may have resulted from heating effects in the open-path infrared gas analyzer (Burba et al., 2008). We recently created a Li-Cor LI-8150 gas analyzer system with six long-term monitoring chambers in the footprint area for the eddy covariance measurements, which we will use to test whether that hypothesis is correct.

4.2 Impacts of the environment on NEE, GPP, and R_{ec}

Understanding the relationships between precipitation patterns and inter-annual variations of carbon flux is an important step towards predicting how future climate change will affect carbon cycles in arid and semiarid ecosystems (Poulter et al., 2014; Scott et al., 2014; Liu et al., 2016a). Our results demonstrated the important roles of the environmental factors in regulating the direction and amount of NEE between the atmosphere and the ecosystem in a sandy grassland in the Horqin Sandy Land. The dominant environmental factors differed among seasons at the different scales (Nakano et al., 2008; Ueyama et al., 2010).

At an annual scale, the amount of precipitation was the dominant factor in regulating the annual carbon exchange of this sandy grassland. NEE was negatively linearly related to precipitation on an annual basis (Fig. 6). This result is consistent with data

from a northern temperate grassland in Canada (Flanagan et al., 2002) and a tallgrass prairie in the United States (Suyker et al., 2003). Annual herbaceous plants are vulnerable to decreased precipitation, which decreases their productivity by reducing stomatal conductance and leaf area, while simultaneously increasing the soil water deficit (Ford et al., 2008). Soil water deficits and decreased substrate availability for soil microbes can also decrease R_{ec} (Shi et al., 2014). In addition, GPP generally responds more strongly than R_{ec} to drought in arid and semiarid areas (Schwalm et al., 2010; Litvak et al., 2015; Delgado-Balbuena et al., 2019). Our result was consistent with these studies, as the slope of the regression line that relates precipitation to GPP (0.98) was much higher than that for R_{ec} (0.51) (Fig. 6). However, we must improve our understanding of the responses of the ecosystem to precipitation and the underlying mechanisms that control whether it will be a carbon source or sink. To accomplish this, it will be necessary to observe the ecosystem continuously for a longer period of time.

The dominant factors varied seasonally. In the spring, NEE was most strongly affected by T_{soil} (Fig. 8), SWC (Fig. 8), and the amount of precipitation (Fig. 7). After experiencing the winter cold and drought, GPP and R_{ec} increased with increasing temperature and precipitation during the spring (Chu et al., 2013; Wolf et al., 2016). In the present study, NEE was negatively related to the amount of precipitation (Fig. 7), which suggests that spring precipitation leads to increased ecosystem carbon uptake in sandy grassland, likely because the water replenishes the soil water storage in time to facilitate the emergence and growth of shallow-rooted annual plants (Scott et al., 2000; Liu et al., 2016a). In turn, this increases ecosystem CO_2 uptake. Therefore, spring precipitation results in greater emergence and growth of annuals, which leads to a higher contribution of this season to the ecosystem productivity (Huang et al, 2015).

In semiarid ecosystems such as our study site, summer precipitation supplies the majority of the annual precipitation and soil moisture for most of the annual plant growth (Emmerich and Verdugo, 2008; Sun et al., 2015). Our results showed that NEE was significantly negatively correlated with SWC from 40 to 50 cm. This is likely to be related to the size and frequency of each precipitation event. For example, events

with high precipitation (>20 mm) occurred five times in 2018, versus not at all in 2015 and once in 2016 (Table 1), and the carbon uptake in 2018 was higher than that in 2015 and 2016 (Fig. 4b). Effective precipitation may penetrate deeper into the soil, thereby recharging soil water in deeper layers, which stimulates plant growth and carbon absorption (Harper et al., 2005; Bell et al., 2012); on the other hand, the water can potentially move below the rooting zone and become unavailable to plants. However, our results indicated that the relationship between SWC from 0 to 10 cm and NEE was not significant. The near-surface SWC would be closely linked to small precipitation amounts (<5 mm) (Fig. 2). Studies suggest that small precipitation amounts may be intercepted by the plant canopy or may replenish only the near-surface soil, where water may evaporate before plants can take advantage of it, thereby reducing its impact on NEE (Schwinning and Sala, 2004; Hao et al., 2010). Therefore, the effective precipitation events appear to be more efficient than small precipitation events for regulating NEE in sandy grassland in the summer.

In the autumn, NEE increased with increasing T_{soil} and SWC from 0 to 10 cm (Fig. 8). As was the case in the summer, the near-surface SWC was closely related to small precipitation events (<5 mm). However, unlike in the summer, autumn is cooler and miosture evaporates more slowly from the near-surface soil, and microbial respiration is sensitive to precipitation when the temperature is suitable for microbial activity in semiarid regions (Huxman et al., 2004; Sponseller, 2006; Roby et al., 2019). Thus, small rainfall events can stimulate ecosystem CO_2 loss chiefly through their effect on microbial respiration (Reynolds et al., 2004; Hao et al., 2010). However, the relationship between NEE and SWC in deeper soil layers was negative (Fig. 8c), which was similar to the relationship in summer.

In winter, the annual plants had withered, so there was no GPP and the entire ecosystem was characterized by carbon emission (Morgner et al., 2010; Gao et al., 2012). Our results showed that NEE increased with decreasing SWC and temperature (Table S1). Previous studies found that when SWC decreases sufficiently to create water stress, it may replace temperature as the main factor that controls soil respiration

in arid and semiarid areas in winter (Wu et al., 2010; Escolar et al., 2015), and as a result, soil respiration decreased with decreasing SWC (Manzoni et al., 2011; Oikawa et al., 2011). Our results were inconsistent with these previous studies. This may be due to the effects of drought, since precipitation during the winter amounted to between 1 and 6 % of the annual precipitation, and this drought would be exacerbated by strong winter winds in the Horqin Sandy Land (Fig. S5; Wang et al., 2005; Liu et al., 2016b). The soil organic matter and nutrients would also be lost faster when SWC decreases and the wind strengthens, resulting in increased carbon emission (Lal, 2004; Munodawafa, 2011).

5 Conclusions

Our field data indicated that the sandy grassland has functioned as a net CO_2 source at an annual scale, with a mean annual NEE of 49 ±8 g C m^{-2} yr^{-1}. At the seasonal scale, the sandy grassland showed net CO_2 absorption during the summer, but net CO_2 release in the other seasons. At the diurnal scale, the ecosystem showed a strong single daytime absorption peak in the spring and summer, but strong CO_2 emission at night. In autumn and winter, the ecosystem was characterized by CO_2 emission throughout the day.

Annual precipitation was significantly negatively correlated with NEE. Seasonally, NEE was mainly affected by T_{soil} and the amount of precipitation in the spring, by the frequency and amount of effective precipitation events in summer, by T_{soil} and SWC at all depths in autumn, and by T_{soil} at all depths and SWC from 30 to 50 in winter. Our findings demonstrated the importance of long-term, high-frequency field monitoring in sandy land to improve our understanding of CO_2 cycling and its likely responses to a changing climate. However, it will be necessary to study the NEE for a longer period to reveal its long-term response to environmental and biological factors and learn when the ecosystem will recover sufficiently to become a net carbon sink on an annual basis.

Data availability. In agreement with the FAIR Data standards, the data used in this article are archived, published, and available in a dedicated repository: http://doi.org/10.4121/uuid:35deeb02-8165-49b7-af8d-160d537ae15a.

Competing interests. The authors declare that they have no conflict of interest.

Author contributions. YQL, YYN, HBY, XYW, and YLD designed the study; YYN, XWG, and JL performed the experiments. YYN and HBY analyzed the data. YYN drafted the manuscript. All co-authors had a chance to review the manuscript and contributed to discussion and interpretation of the data.

Acknowledgements. This research was supported by the National Key Research and Development Program of China (2017YFA0604803 and 2016YFC0500901), the National Natural Science Foundation of China (grants 31971466, 31560161, 31260089, and 31400392), the Chinese Academy of Sciences "Light of West China" Program (18JR3RA004), and the One Hundred Person Project of the Chinese Academy of Sciences (Y551821).

References

Asner, G. P., Archer, S., Hughes, R. F., Ansley, R. J., and Wessman, C. A.: Net changes in regional woody vegetation cover and carbon storage in Texas Drylands, 1937–1999, Glob. Change Biol., 9, 316–335, https://doi.org/10.1046/j.1365-2486.2003.00594.x, 2003.

Bagan, H., Takeuchi, W., Kinoshita, T., and Bao, Y. H.: Land cover classification and change analysis in the Horqin Sandy Land from 1975 to 2007, IEEE J. Sel. Topics in Applied Earth Observations and Remote Sensing, 3, 168-177. https://doi.org/10.1109/jstars.2010.2046627, 2010.

Baldocchi, D., Falage, E., Gu, L, H., Olson, R., Hollinger, D., Running, S., Anthoni, P., Bernhofer, C., Davis, K., Evans, R., Fuentes, J., Goldstein, A., Katul, G., Law, B., Lee, X. H., Malhi, Y., Meyers, T., Munger, W., Oechel, W., Paw, U. K. T., Pilegaard, K., Schmid, H. P., Valentini, R., Verma, S., Vesala, T., Wilson, K., and Wofsy, S.: Fluxnet: a new tool to study the temporal and spatial variability of ecosystem-scale carbon dioxide, water vapor, and energy flux densities, Bulletin of the American Meteorological Society., 82, 2415–2434. https://doi.org/10.1175/1520-0477(2001)082<2415:FANTTS>2.3.CO;2, 2001.

Barrett, G. W.: The effects of an acute insecticide stress on a semi-enclosed grassland ecosystem, Ecology, 49, 1019, https://doi.org/10.2307/1934487, 1968.

Bell, T. W., Menzer, O., Troyo-Diequez, E., and Oechel, W. C.: Carbon dioxide exchange over multiple temporal scales in an arid shrub ecosystem near La Paz,

Baja California Sur, Mexico. Glob. Change Biol., 18, 2570–2582. https://doi.org/10.1111/j.1365-2486.2012.02720.x, 2012.

Biederman, J. A., Scott, R. L., Bell, T. W., Bowling. D. R., Dore, S., Garatuza-Payan, J., Kolb, T. E., Krishnan, P., Krofchec, D. J., Litv, M E., Maurer, G. E., Meyers, T. P., Oechel, W. C., Papuga, S. A., Ponce-Campos, G. E., Rodriguez, J. C., Smith, W. K., Vargas, R., Watts, C. J., Yepez, E. A., and Goulden, M. L.: CO_2 exchange and evapotranspiration across dryland ecosystems of southwestern North America. Glob. Change Biol., 23, 4204–4221. https://doi.org/10.1111/gcb.13686, 2017.

Biederman, J. A., Scott, R. L., Goulden, M. L., Vargas, R., Litvak, M. E., Kolb, T. E., Yepez, E. A., Oechel, W. C., Blanken, P. D., Bell, T. W., Garatuza-Payan, J., Maurer, G. E., Dore, S., and Burns, S. P.: Terrestrial carbon balance in a drier world: the effects of water availability in southwestern North America. Glob. Change Biol., 22, 1867-1879. https://doi.org/110.1111/gcb.13222, 2016.

Burba, G. G., McDermitt, D. K., Grelle, A., and Daniel, J. A.: Addressing the influence of instrument surface heat exchange on the measurements of CO_2 flux from open-path gas analyzers, Glob. Change Biol., 14, 1854-1876, https://doi.org/10.1111/j.1365-2486.2008.01606.x, 2008.

Chu, J. M., Wang, Q., Fan, Z. P., and Li, F. Y.: Effects of soil moisture condition and freeze-thaw cycle on soil respiration of different land-use types in Horqin Sandy Land, Chinese J. Ecol., (in Chinese), 32, 1399-1404, http://www.cje.net.cn/EN/, 2013.

Ciais, P. H., Reichstein, M., Viovy, N., Granier, A., Ogée, J., Allard, V., Aubinet, M., Buchmann, N., Bernhofer, C., Carrara, A., Chevallier, F., Noblet, N. D., Friend, A. D., Friedlingstein, P., Grünwald, T., Heinesch, B., Keronen, P., Knohl, A., Krinner, G., Loustau, D., Manca, G., Matteucci, G., Miglietta, F., Ourcival, J. M., Papale, D., Pilegaard, K., Rambal, S., Seufert, G., Soussana, J. F., Sanz, M. J., Schulze, E. D., Vesala, T., and Valentini, R.: Europe-wide reduction in primary productivity caused by the heat and drought in 2003, Nature, 437, 529-533, https://doi.org/10.1038/nature03972, 2005.

Cleverly, J., Boulain, N., Villalobos-Vega, R., Grant, N., Faux, R., Wood, C., Cook, P.

G., Yu, Q., Leigh, A., and Eamus, D.: Dynamics of component carbon fluxes in a semi-arid Acacia woodland, central Australia, JGR Biogeosciences., 118, 1168–1185, http://dx.doi.org/10.1002/jgrg.20101, 2013.

Cleverly, J., Eamus, D., Gorsel, E. V., Chen, C., Rumman, R., Luo, Q. Y., Coupe, N. R., Li, L. H., Kljun, N., Faux, R., Yu, Q., and Huete, A.: Productivity and evapotranspiration of two contrasting semiarid ecosystems following the 2011 global carbon land sink anomaly, Agric. For. Meteorol., 220, 151-159. https://doi.org/10.1016/j.agrformet.2016.01.086, 2016.

Czobel, S., Szirmai, O., Nemeth, Z., Gyuricza, C., Házi, J., Tóth, A., Schellenberger, J., Vasa, L., and Penksza, K.: Short-term effects of grazing exclusion on net ecosystem CO_2 exchange and net primary production in a Pannonian sandy grassland, Notulae Botanicae Horti Agrobotanici Cluj-Napoca, 40, 67-72, https://doi.org/10.15835/nbha4028300, 2012.

Delgado-Balbuena, J., Arredondo, J. T., Loescher, H. W., Pineda-Martínez, L. F., Carbajal, J. N., and Vargas, R.: Seasonal precipitation legacy effects determine the carbon balance of a semiarid grassland, JGR Biogeosciences, 124, 987-1000, https://doi.org/10.1029/2018JG004799, 2019.

Delpierre, N., Soudani, K., Francois, C., Pontailler, J. Y., Nikinmaa, E., Misson, L., Aubinet, M., Bernhofer, C., Granier, A., Grünwald, T., Heinesch, B., Longdoz, B., Ourcival, J. M., Rambal, S., Vesala, T., and Dufrene, E.: Exceptional carbon uptake in European forests during the 2007 warm spring: a data- model analysis, Glob. Change Biol., 15, 1455-1474. https://doi.org/10.1111/j.1365-2486.2008.01835.x, 2010.

Emmerich, W. E.: Carbon dioxide fluxes in a semiarid environment with high carbonate soils, Agric. For. Meteorol., 116, 91–102, https://doi.org/10.1016/s0168-1923(02)00231-9, 2003.

Emmerich, W. E., and Verdugo, C. L.: Precipitation thresholds for CO_2 uptake in grass and shrub plant communities on Walnut Gulch Experimental Watershed, Water Resour. Res., 44, 435-443. https://doi.org/10.1029/2006wr005690, 2008.

Escolar, C., Maestre, F. T , and Rey. A.: Biocrusts modulate warming and rainfall exclusion effects on soil respiration in a semi-arid grassland, Soil Biol. Biochem., 80, 9-17, https://doi.org/10.1016/j.soilbio.2014.09.019, 2015.

633 Falge, E., Baldocchi, D., Olson, R., Anthoni, P., and Dolman, H.: Gap filling strategies
634 for defensible annual sums of net ecosystem exchange, Agric. For. Meteorol.,
635 107, 43-69, https://doi.org/10.1016/S0168-1923(00)00225-2, 2001.
636 Fang, S. X., Zhou, L. X., Tans, P. P., Ciais, P., Steinbacher, M., Xu, L., and Luan, T.: *In*
637 *situ* measurement of atmospheric CO_2 at the four WMO/GAW stations in China,
638 Atmos. Chem. Phys., 14, 27287-27326. https://doi.org/10.5194/acp-14-2541-
639 2014, 2014.
640 Flanagan, L. B., Wever, L. A., Carlson, P. J., Seasonal and interannual variation in
641 carbon dioxide exchange and carbon balance in a northern temperate grassland,
642 Glob. Change Biol., 8, 599–615. http://dx.doi.org/10.1046/j.1365-
643 2486.2002.00491.x, 2002.
644 Ford, C. R., Mitchell, R. J., and Teskey, R. O.: Water table depth affects productivity,
645 water use, and the response to nitrogen addition in a savanna system. Can. J. For.
646 Res., 38, 2118-2127. https://doi.org/10.1139/X08-061, 2008.
647 Gang, C. C., Zhang, J., and Li, J. L.: The advances in the carbon source/sink researches
648 of typical grassland ecosystem in China, Procedia Environ. Sci., 10, 1646-1653.
649 https://doi.org/10.1016/j.proenv.2011.09.259, 2011.
650 Gao, Y. H., Li, X. R., Liu, L. C., Jia, R. L., Yang, H. T., Li, G., and Wei, Y. P.: Seasonal
651 variation of carbon exchange from a revegetation area in a Chinese desert, Agric.
652 For. Meteorol., 156, 134-142, https://doi.org/10.1016/j.agrformet.2012.01.007,
653 2012.
654 Hair, J. F., Black, B., Babin, B., Anderson, R. E., and Tatham, R. L.: Multivariate data
655 analysis, 6th Ed. New Jersey: Prentice Hall, 2005.
656 Hao, Y. B., Wang, Y. F., Mei, X., and Cui, X. R.: The response of ecosystem CO_2
657 exchange to small precipitation pulses over a temperate steppe. Plant Ecol., 209,
658 335-347. https://doi.org/10.1007/s11258-010-9766-1, 2010.
659 Harper, C. W., Blair, J. M., Fay, P. A., Knapp, A. K., and Carlisle, J. D.: Increased
660 rainfall variability and reduced rainfall amount decreases soil CO_2 flux in a
661 grassland ecosystem. Glob. Change Biol., 11, 322–334.
662 https://doi.org/10.1111/j.1365-2486.2005.00899.x, 2005.
663 Hastings, S. J., Oechel, W. C., and Muhliamelo, A.: Diurnal, seasonal and annual
664 variation in the net ecosystem CO_2 exchange of a desert shrub community

(sarcocaulescent) in Baja California, Mexico. Glob. Change Biol., 11, 927-939, https://doi.org/10.1111/j.1365-2486.2005.00951.x, 2010.

Huang, G., Li, Y., and Collins, B.: Phenological transition dictates the seasonal dynamics of ecosystem carbon exchange in a desert steppe, J. Veg. Sci., 26, 337-347. http://dx.doi.org/10.1111/jvs.12236, 2015.

Huenneke, L. F., Anderson, J. P., Remmenga, M., and Schlesinger, W. H.: Desertification alters patterns of aboveground net primary production in Chihuahuan ecosystems, Glob. Change Biol., 8, 247-264. https://doi.org/10.1046/j.1365-2486.2002.00473.x, 2002.

Hutley, L. B., Leuning, R., Beringer, J., and Cleugh, H. A.: The utility of the eddy covariance techniques as a tool in carbon accounting: tropical savanna as a case study, Austral. J. Bot., 53, 663. https://doi.org/10.1071/Bt04147, 2005.

Huxman, T. E., Snyder, K. A., Tissue, D., Leffler, A. J., Ogle, K., Pockman, W. T., Sandquist, D. R., Potts, D. L., and Schwinning, S.: Precipitation pulses and carbon fluxes in semiarid and arid ecosystems, Oecologia, 141, 254–268, https://doi.org/10.1007/s00442-004-1682-4, 2004.

Jia, X., Zha, T. S., Wu, B., Zhang, Y. Q., Gong, J. N., Qin, S. G., Chen, G. P., Kellomäki, S., and Peltola, H.: Biophysical controls on net ecosystem CO_2 exchange over a semiarid shrubland in northwest China, Biogeosciences, 11, 4679-4693. https://doi.org/ 10.5194/bg-11-4679-2014, 2014.

Jongen, M., Pereira, J. S., Aires, L. M. I., and Pio, C. A.: The effects of drought and timing of precipitation on the inter-annual variation in ecosystem-atmosphere exchange in a mediterranean grassland. Agric. For. Meteorol., 151, 595-606, https://doi.org/10.1016/j.agrformet.2011.01.008, 2011.

Joseph Turk, F., Pasadena, J. P. L., Li, L., and Haddad, Z. S.: Physical modeling of microwave surface emissivity from passive microwave satellite observations room 256 (New Orleans Convention Center), 2012.

Kang, W. P., Wang. T., and Liu. S. L.: The response of vegetation phenology and productivity to drought in semi-arid regions of Northern China, Remote Sensing., 10, 727. https://doi.org/10.3390/rs10050727, 2018.

Keenan, T., Garcá, R., Friend, A. D., Zaehle, S., Sabate, S.: Improved understanding of drought controls on seasonal variation in Mediterranean forest canopy CO_2

and water fluxes through combined *in situ* measurements and ecosystem modelling, Biogeosci. Discuss., 6, 2285-2329, https: https://doi.org/10.5194/bgd-6-2285-2009, 2009.

Kemp, P. R.: Phenological patterns of Chihuahuan desert plants in relation to the timing of water availability, J. Ecol., 71, 427-436. https://doi.org/10.2307/2259725, 1983.

Kiely, G., Leahy, P., Sottocornola, M., Laine, A., Mishurov, M., Albertson, J., and Carton, O.: Celticflux: measurement and modelling of greenhouse gas fluxes from grasslands and a peatland in Ireland. Irish Environmental Protection Agency, STRIVE Report 24, http://www.epa.ie/pubs/reports/research/climate/strivereport24.html, 2009.

Knorr, W., Prentice, I. C., House, J. I., and Holland, E. A.: Long-term sensitivity of soil carbon turnover to warming, Nature, 433, 298–301. https://doi.org/10.1038/nature03226, 2005.

Lal, R.: Potential of desertification control to sequester carbon and mitigate the greenhouse effect, Clim. Change, 51, 35–72. https://doi.org/110.1023/a:1017529816140, 2001.

Lal, R.: Carbon sequestration in dryland ecosystems, Environ. Manage., 33, 528–544. https://doi.org/10.1007/s00267-003-9110-9, 2004.

Lee, X. H., Massman, W. J., and Law, B. E.: Handbook of micrometeorology, Springer, Berlin. Vol. 29 of the Atmospheric and Oceanographic Sciences Library, https://doi.org/10.1007/1-4020-2265-4, 2004.

Li, L., Wang, Y. P., Beringer, J., Shi, H., Cleverly, J., Cheng, L., Eamus, D., Huete, A., Hutley, L., Lu, X. J., Piao, S. L., and Zhang, L.: Responses of LAI to rainfall explain contrasting sensitivities to carbon uptake between forest and non-forest ecosystems in Australia, Scientific Reports, 7, 11720. https://doi.org/10.1038/s41598-017-11063-w, 2017.

Li, R. P., and Zhou, G. S.: A temperature-precipitation based leafing model and its application in Northeast China, Plos One., 7, e33192. https://doi.org/10.1371/journal.pone.0033192, 2012.

Li, Y. Q., Wang X. Y., Chen, Y. P., Luo, Y. Q., Lian, J., Niu, Y. Y., Gong, X. W., Yang, H., and Yu, P. D.: Changes in surface soil organic carbon in semiarid degraded

729 Horqin Grassland of northeastern China between the 1980s and the 2010s,
730 Catena, 174, 217–226, https://doi.org/10.1016/j.catena.2018.11.021, 2019.
731 Li, Y. Q., Zhang, J. P., Zhao, X. Y., Zhang, T. H., Li, Y. L., Liu, X. P. , and Chen, Y. P.:
732 Comparison of soil physico-chemical properties under different land-use and
733 cover types in northeastern China's Horqin Sandy Land, Sciences in Cold and
734 Arid Regions., 8, 495-506. https://doi.org/ 10.3724/SP.J.1226.2016.00495, 2016.
735 Li, Y. Q., Zhao, X. Y., Chen, Y. P., Luo, Y. Q., and Wang, S. K.: Effects of grazing
736 exclusion on carbon sequestration and the associated vegetation and soil
737 characteristics at a semi-arid desertified sandy site in Inner Mongolia, northern
738 China, Can. J. Soil Sci., 92, 807-819, https://doi.org/10.4141/cjss2012-030, 2012.
739 Li, Y. Q., Zhao, X. Y., Wang, S. K., Zhang, F. X., Lian, J., Huang, W. D., and Qu, H.:
740 Carbon accumulation in the bulk soil and different soil fractions during the
741 rehabilitation of desertified grassland in Horqin Sandy Land (northern China),
742 Pol. J. Ecol., 63, 88-101, https://doi.org/10.3161/15052249PJE2015.63.1.008,
743 2015.
744 Litvak, M. E., Krofcheck, D. J., and Maurer, G.: Quantifying the resilience of carbon
745 dynamics in semi-arid biomes in the Southwestern U.S. to drought, Am. Geophys.
746 Union Fall. Meeting. Abstract, 2015.
747 Liu, R., Cieraad, E., Li, Y., and Ma, J. J. E.: Precipitation pattern determines the inter-
748 annual variation of herbaceous layer and carbon fluxes in a phreatophyte-
749 dominated desert ecosystem, Ecosystems, 19, 601-614,
750 https://doi.org/10.1007/s10021-015-9954-x, 2016a.
751 Liu, S. L., Kang, W. P., and Wang, T.: Drought variability in Inner Mongolia of northern
752 China during 1960–2013 based on standardized precipitation evapotranspiration
753 index, Environ. Earth Sci., 75, 145. https://doi.org/10.1007/s12665-015-4996-0,
754 2016b.
755 Lloyd, J., and Taylor, J. A.: On the temperature dependence of soil respiration,
756 Functional Ecology, 8, 315-323, https://doi.org/10.2307/2389824, 1994.
757 Ma, S. Y., Baldocchi, D. D., Xu, L. K., and Hehn, T.: Inter-annual variability in carbon
758 dioxide exchange of an oak/grass savanna and open grassland in California.
759 Agric. For. Meteorol., 147, 157-171,
760 https://doi.org/10.1016/j.agrformet.2007.07.008, 2007.
761 Manzoni, S., Schimel, J. P., and Porporato, A.: Physical vs. physiological controls on

762 water-stress in soil microbial communities, 96th ESA Annual Convention 2011.
763 https://doi.org/10.1890/11-0026.1, 2011.
764 Morgner, E., Elberling, B., Strebel, D., and Cooper, E. J.: The importance of winter in
765 annual ecosystem respiration in the high arctic: effects of snow depth in two
766 vegetation types, Polar Research, 29, 58-74. https://doi.org/10.1111/j.1751-
767 8369.2010.00151.x, 2010.
768 Munkhdalai, Z. A., Feng, Z. W., Wang, X. K., and Sun, H. W.: Sandy grassland
769 blowouts in Hulunbuir, northeast China: geomorphology, distribution, and causes,
770 Progress in Natural Science: Materials International, 17, 68-73.
771 https://doi.org/10.1080/10020070612331343227, 2007.
772 Munodawafa, A.: Maize grain yield as affected by the severity of soil erosion under
773 semi-arid conditions and granitic sandy soils of Zimbabwe, Physics and
774 Chemistry of the Earth Parts A/B/C, 36, 963-967,
775 https://doi.org/10.1016/j.pce.2011.07.068, 2011.
776 Mureithi, S. M., Verdoodt, A., and Ranst, E. V.: Effects and implications of enclosures
777 for rehabilitating degraded semi-arid rangelands: critical lessons from Lake
778 Baringo Basin, Kenya, Land Degradation and Desertification: Assessment,
779 Mitigation and Remediation, https://doi.org/10.1007/978-90-481-8657-0_9,
780 2010.
781 Nakano, T., Nemoto, M., and Shinoda, M.: Environmental controls on photosynthetic
782 production and ecosystem respiration in semi-arid grasslands of Mongolia, Agric.
783 For. Meteorol., 148, 1456-1466, https://doi.org/10.1016/j.agrformet.2008.04.011,
784 2008.
785 Niu, S, L., Luo, Y, Q., Fei, S, F., and Montagnani, L.: Seasonal hysteresis of net
786 ecosystem exchange in response to temperature change: patterns and causes,
787 Glob. Change Biol., 17, 3102-3114, https://doi.org/10.1111/j.1365-
788 2486.2011.02459.x, 2011.
789 Niu, Y. Y., Li, Y. Q., Wang, X. Y., Gong, X. W., Luo, Y. Q., and Tian, D.Y.:
790 Characteristics of annual variation in net carbon dioxide flux in a sandy grassland
791 ecosystem during dry years. Acta Prataculturae Sinica (in Chinese), 27, 215-221,
792 https://doi.org/10.11686/cyxb2017231, 2018.
793 Nosetto, M. D., Jobbágy, E. G., and Paruelo, J. M.: Carbon sequestration in semi-arid
794 rangelands: comparison of *Pinus ponderosa* plantations and grazing exclusion in
795 NW Patagonia, J. Arid Environ., 67, 142-156,

https://doi.org/10.1016/j.jaridenv.2005.12.008, 2006.

Oikawa, P., Grantz, D. A., and Jenerette, D.: Variation in the temperature sensitivity of heterotrophic soil respiration in response to pulse water events and substrate limitation. Am. Geophys. Union Fall. Meeting. Abstract, 2011.

Petrie, M. D., Collins, S. L., Swann, A. M., Ford, P. L., and Litvak, M. E.: Grassland to shrubland state transitions enhance carbon sequestration in the northern Chihuahuan desert, Glob. Change Biol., 21, 1226-1235. http://dx.doi.org/10.1111/gcb.12743, 2015.

Ponce Campos, G. E., Moran, M. S., Huete, A., Zhang, Y., Bresloff, C., Huxman, T. E., Eamus, D., Bosch, D. D., Buda, A. R., Gunter, S. A., Scalley, T. H., Kitchen, S. G., McClaran, M. P., McNab, W. H., Montoya, D. S., Morgan, J. A., Peters, D. P. C., Sadler, E. J., Seyfried, M. S., and Starks, P. J.: Ecosystem resilience despite large-scale altered hydroclimate conditions, Nature, 494, 349–352, http://dx.doi.org/10.1038/nature11836, 2013.

Poulter, B., Frank, D., Ciais, P., Myneni, R. B., Andela, N., Bi, J., Broquet, G., Canadell, J. G., Chevallier, F., and Liu, Y. Y.: Contribution of semi-arid ecosystems to interannual variability of the global carbon cycle, Nature, 509, 600–603, https://doi.org/10.1038/nature13376, 2014.

Prevéy, J. S., Seastedt, T. R., and Wilson, S.: Seasonality of precipitation interacts with exotic species to alter composition and phenology of a semi-arid grassland. J. Ecol., 102, 1549-1561. https://doi.org/10.1111/1365-2745.12320, 2014.

Reichstein, M., Falge, E., Baldocchi, D., Papale, D., Aubinet, M., Berbigier, P., Bernhofer, C., Buchmann, N., Gilmanov, T., and Granier, A.: On the separation of net ecosystem exchange into assimilation and ecosystem respiration: review and improved algorithm. Glob. Change Biol., 11, 1424-1439. https://doi.org/10.1111/j.1365-2486.2005.001002.x, 2005.

Rey, A., Pegoraro, E., Oyonarte, C., Were, A., Escribano, P., and Raimundo, J.: Impact of land degradation on soil respiration in a steppe (*Stipa tenacissima* L.) semi-arid ecosystem in the SE of Spain, Soil Biol. Biochem., 43, 393-403. https://doi.org/10.1016/j.soilbio.2010.11.007, 2011.

Reynolds, J. F., Kemp, P. R., Ogle, K., and Fernandez, R. J.: Modifying the “pulse-

reserve" paradigm for deserts of North America: precipitation pulses, soil water and plant responses, Oecologia, 141, 194–210. https://doi.org/10.2307/40005681, 2004.

Roby, M. C., Scott, R. L., Barron-Gafford, G. A., Hamerlynck, E. P., and Moore, D. J. P.: Environmental and vegetative controls on soil CO_2 efflux in three semiarid ecosystems, Soil Systems, 3, 6. https://doi.org/10.3390/soilsystems3010006, 2019.

Ruiz-Jaen, M, C., and Aide, T. M.: Restoration success: how is it being measured? Restor. Ecol., 13, 569-577, https://doi.org/10.1111/j.1526-100X.2005.00072.x, 2005.

Sala, O. E., Parton, W. J., Joyce, L. A., and Lauenroth, W.K.: Primary production of the central grassland region of the United States, Ecology, 69, 40–45. https://doi.org/10.2307/1943158, 1988.

Schmid, H. P.: Experimental design for flux measurements: matching scales of observations and fluxes. Agric. For. Meteorol., 87, 179-200. http://dx.doi.org/10.1016/S0168-1923(97)00011-7, 1997.

Schwalm, C. R., Williams, C. A., Schaefer, K., Arneth, A., Bonal, D., Buchmann, N., Chen, J., Law, B. E., Lindroth, A., Luyssaert, S., Reichstein, M., and Richardson, A. D.: Assimilation exceeds respiration sensitivity to drought: a FLUXNET synthesis, Glob. Change Biol., 16, 657–670, https://doi.org/10.1111/j.1365-2486.2009.01991.x, 2010.

Schwinning, S., and Sala, O. E., Hierarchy of responses to resource pulses in arid and semi-arid ecosystems, Oecologia., 141, 211–220. https://doi.org/10.2307/40005682, 2004.

Scott, R. L., Biederman, J. A., Hamerlynck, E. P., and Barron-Gafford, G. A.: The carbon balance pivot point of southwestern U.S. semiarid ecosystems: insights from the 21st century drought, JGR Biogeosciences, 120, 2612-2624. https://doi.org/110.1002/2015JG003181, 2015.

Scott, R. L., Jenerette, G. D., Potts, D. L., and Huxman, T. E.: Effects of seasonal drought on net carbon dioxide exchange from a woody-plant-encroached semiarid grassland, JGR Biogeosciences, 114, G04004.

https://doi.org/10.1029/2008jg000900, 2009.

Scott, R. L., Shuttleworth, W. J., Goodrich, D. C., and Maddock, T.: The water use of two dominant vegetation communities in a semiarid riparian ecosystem, Agric. For. Meteorol., 105, 241–256. http://dx.doi.org/10.1016/s0168-1923(00)00181-7, 2000.

Scott R. L., Huxman, T. E., Barron-Gafford, G. A., Jenerette, G. D., Young, J. M., and Hamerlynck, E. P.: When vegetation change alters ecosystem water availability, Glob. Change Biol., 20, 2198–2210. http://dx.doi.org/10.1111/gcb.12511, 2014.

Shachak, M., Sachs, M., and Moshe, I.: Ecosystem management of desertified shrublands in Israel, Ecosystems, 1, 475-483. https://doi.org/10.1007/s100219900043, 1998.

Shen, M. G., Piao, S. L., Cong, N., Zhang, G.X., and Jassens, I. A.: Precipitation impacts on vegetation spring phenology on the Tibetan Plateau. Glob. Change Biol., 21, 3647-3656. https://doi.org/10.1111/gcb.12961, 2015.

Shi, Z., Thomey, M. L., Mowll, W., and Litvak, M.: Differential effects of extreme drought on production and respiration: synthesis and modeling analysis, Biogeosciences, 11, 621-633. https://doi.org/10.5194/bg-11-621-2014, 2014.

Sousa, F. P., Ferreira, T. O., Mendonça, E. S., Romero, R. E., and Oliveira, J. G. B.: Carbon and nitrogen in degraded Brazilian semi-arid soils undergoing desertification, Agric. Ecosyst. Environ., 148, 11-21. https://doi.org/10.1016/j.agee.2011.11.009, 2012.

Sponseller, R. A.: Precipitation pulses and soil CO_2 flux in a Sonoran Desert ecosystem, Glob. Change Biol., 13, 426–436. https://doi.org/10.1111/j.1365-2486.2006.01307.x, 2006.

Su, Y. Z., Zhao, H. L., and Zhang, T. H.: Influence of grazing and enclosure on carbon sequestration in degraded sandy grassland, Inner Mongolia, North China. J. Environ. Sci., (In Chinese), 46, 321-328. https://doi.org/10.1080/00288233.2003.9513560, 2003.

Sun, D. C., Li, Y. L., Zhao, X. Y., Zuo, X. A., and Mao, W.: Effects of enclosure and grazing on carbon and water fluxes of sandy grassland, Chinese Journal of Plant Ecology (in Chinese), 39, 565-576. https://doi.org/10.17521/cjpe.2015.0054, 2015.

890 Suyker, E. A., Verma, S. B., Burba, G. G.: Inter-annual variability in net CO_2 fluxes
891 exchange of a native tallgrass prairie, Glob. Change Biol., 9, 255–265.
892 http://dx.doi.org/10.1046/j.1365-2486.2003.00567.x, 2003.
893 Ueyama, M., Ichii, K,, Hirata, R., Takagi, K., Asanuma, J., Machimura, T., Nakai, Y.,
894 Ohta, T., Saigusa, N., Takahashi, Y., and Hirano, T.: Simulating carbon and water
895 cycles of larch forests in East Asia by the BIOME-BGC model with AsiaFlux
896 data, Biogeosciences, 7, 959-977. https://doi.org/ 10.5194/bg-7-959-2010, 2010.
897 Vest, K. R., Elmore, A. J, Kaste, J. M., and Okin, G. S.: Functional connectivity as a
898 possible indicator of desertification in degraded grasslands, Am. Geophys. Union
899 Fall. Meeting. Abstract B51A-0383, 2011.
900 Wagle, P., and Kakani, V. G.: Environmental control of daytime net ecosystem
901 exchange of carbon dioxide in switchgrass, Agric. Ecosyst. Environ., 186, 170-
902 177, https://doi.org/10.1016/j.agee.2014.01.028, 2014.
903 Wang, X. M., Dong, Z. B., Yan, P., Zhang, J. Z., and Qian, G. Q.: Wind energy
904 environments and dunefield activity in the Chinese deserts, Geomorphology, 65,
905 33-48, https://doi.org/10.1016/j.geomorph.2004.06.009, 2005.
906 Webb, E. K., Pearman, G. I., and Leuning, R.: Correction of flux measurements for
907 density effects due to heat and water vapor transfer, Q. J. Roy. Meteorol. Soc.,
908 106, 85-100, https://doi.org /10.1002/qj.49710644707, 1980,
909 Webb, W., Szarek, S., Lauenroth, W., Kinerson, R., and Smith, M.: Primary productivity
910 and water use in native forest, grassland, and desert ecosystem, Ecology, 59,
911 1239–1247, https://doi.org/10.2307/1938237, 1978.
912 Wohlfahrt, G., Fenstermaker, L. F., and Arnone, J.A. III: Large annual net ecosystem
913 CO_2 uptake of a Mojave Desert ecosystem, Global Change Biol., 14, 1475-1487.
914 https://doi.org/10.1111/j.1365-2486.2008.01593.x, 2008.
915 Wolf, S., Keenan, T. F., Fisher, J. B., Baldocchi, D. D., Desai, A. R., Richardson, A.D.,
916 Scott, R. L., Law, B. E., Litvak, M. E., Brunsell, N. A., Peters, W., and Laan-
917 Luijkx, I. T.: Warm spring reduced carbon cycle impact of the 2012 US summer
918 drought. PNAS, 113, 5880-5885. https://doi.org/10.1073/pnas.1519620113,
919 2016.
920 Wu, C. Y., Chen, J. M., Pumpanen, J., Cescatti, A., Marcolla, B., Blanken, P. D., Ardö,
921 J., Tang, Y. H., Magliulo, V., Georgiadis, T., Soegaard, H., Cook, D. R., and
922 Harding, R. J.: An underestimated role of precipitation frequency in regulating

summer soil moisture. Environ. Res. Lett., 7, 024011. http://dx.doi.org/10.1088/1748-9326/7/2/024011, 2012.

Wu, X., Yao, Z. N., Brüggemann, N., and Shen, Z. Y.: Effects of soil moisture and temperature on CO_2 and CH_4 soil atmosphere exchange of various land use/cover types in a semi-arid grassland in Inner Mongolia, China. Soil Biol. Biochem., 42, 773-787, https://doi.org/10.1016/j.soilbio.2010.01.013, 2010.

Xu, L. K., and Baldocchi, D. D.: Seasonal variation in carbon dioxide exchange over a Mediterranean annual grassland in California, Agric. For. Meteorol., 123, 79-96, https://doi.org/10.1016/j.agrformet.2003.10.004, 2004.

Yan, C. Z., Wang, Y. M., Feng, Y. S., and Wang, J. H.: Macro-scale survey and dynamic studies of sandy land in Ningxia by remote sensing, Journal of Desert Research (in Chinese), 23, 34-37. https://doi.org/1000-694X(2003) 02-0132-04, 2003.

Yun, H. B., Wu, Q. B., Zhuang, Q. L., Chen, A. P., Yu, T., Lyu, Z., Yang, Y. Z., Jin, H. J., Liu, G. J., Qu, Y., and Liu, L. C.: Consumption of atmospheric methane by the Qinghai–Tibet Plateau alpine steppe ecosystem, Cryosphere, 9, 2803-2819. https://doi.org/10.5194/tc-12-2803-2018, 2018.

Zhang, B. W., Li, S., Chen, S. P., Ren, T. T., Yang, Z. Q., Zhao, H. L., Liang, Y., and Han, X. G.: Arbuscular mycorrhizal fungi regulate soil respiration and its response to precipitation change in a semiarid steppe, Sci. Rep., 6, 19990, https://doi.org/10.1038/srep19990, 2016.

Zhao, H. L., Li, Y. Q., and Zhou, R. L.: Effects of desertification on C and N storages in grassland ecosystem on Horqin sandy land, Chinese Journal of Applied Ecology (in Chinese), 18, 2412. https://doi.org/10.1360/yc-007-1324, 2007.

Zhao, W. Z., and Liu, B.: The response of sap flow in shrubs to rainfall pulses in the desert region of China. Agric. For. Meteorol., 150, 1297–1306. https://doi.org/10.1016/j.agrformet.2010.05.012, 2010.

Zhao, W. Z., and Liu, H.: Precipitation pulses and ecosystem responses in arid and semiarid regions: a review, Chinese Journal of Applied Ecology (in Chinese), 22, 243-249. https://doi.org/10.3724/SP.J.1011.2011.00197, 2011.

Zhao, X. Y., Wang, S. K., Luo, Y. Y., Huang, W. D., Qu, H., and Lian, J.: Toward sustainable desertification reversion: a case study in Horqin Sandy Land of northern China. Sciences in Cold and Arid Regions, 1, 23-28.

https://doi.org/10.3724/SP.J.1226.2015.00023, 2015.

Zhao, Y. L., Song, Z. L., Xu, X. T., Li, Z. M., Guo, F. S., and Pan, W. J.: Nitrogen application increases phytolith carbon sequestration in degraded grasslands of North China, Ecol. Res., 31, 117-123, https://doi.org/10.1007/s11284-015-1320-0, 2016.

Zhou, Y. Y., Li, X. R., Gao, Y. H., He, M. Z., Wang, M. M., Wang, Y. L., Zhao, L. N., and Li, Y. F.: Carbon fluxes response of an artificial sand-binding vegetation system to ainfall variation during the growing season in the Tengger Desert, J. Environ. Manage., 266, 110556, https://doi.org/10.1016/j.jenvman.2020.110556, 2020.

966 **Figure captions**

967 **Fig. 1.** (a) Locations of the Horqin Sandy Land and the Naiman station. (b) and (c) are
968 photos of the eddy covariance site at the Naiman station during the growing and
969 dormant seasons, respectively.

970 **Fig. 2.** Changes in soil water content (SWC) at depths of 10, 20, 30, 40, and 50 cm that
971 resulted from precipitation events in spring, summer, and autumn. Precipitation $\geq$ 5 mm
972 represents effective precipitation.

973 **Fig. 3.** Seasonal and inter-annual variation in the daily average net ecosystem CO_2
974 exchange (NEE), gross primary productivity (GPP), and ecosystem respiration (R_{ec})
975 from (a-e) 2014 to 2018. (f) Annual cumulative NEE, GPP and R_{ec} from 2014 to 2018.
976 Positive NEE values indicate net CO_2 release, whereas negative values indicate net CO_2
977 uptake by the ecosystem. Note that the initial measurements were from 15 September
978 to 23 December 2014, so no data are available for the first part of 2014.

979 **Fig. 4.** Seasonal mean net ecosystem CO_2 exchange (NEE), gross primary productivity
980 (GPP), and ecosystem respiration (R_{ec}) from 2014 to 2018: (a) spring (March, April,
981 and May), (b) summer (June, July, and August), (c) autumn (September, October, and
982 November), and (d) winter (December, January, and February). Note that the initial
983 measurements were from 15 September to 23 December 2014, so no data are available
984 for the first part of 2014.

985 **Fig. 5.** Diurnal changes in mean net ecosystem CO_2 exchange (NEE), gross primary
986 productivity (GPP), and ecosystem respiration (R_{ec}) from 2014 to 2018: (a) spring
987 (March, April, and May), (b) summer (June, July, and August), (c) autumn (September,
988 October, and November), and (d) winter (December, January, and February). Note that
989 the initial measurements were from 15 September to 23 December 2014, so the spring
990 and summer data do not include the period before 15 September. The final
991 measurements were obtained on 31 December 2018, so the winter period from 2017 to
992 2018 was only about one-third of the usual length (i.e., it did not include data from
993 January and February 2019).

994 **Fig. 6.** Relationship between annual precipitation and net ecosystem carbon exchange

(NEE), gross primary productivity (GPP), and ecosystem respiration (R_{ec}) for the years with a complete dataset (2015, 2016, and 2018).

Fig. 7. Relationship between monthly net ecosystem carbon exchange (NEE), gross primary productivity (GPP), and ecosystem respiration (R_{ec}) and the corresponding monthly precipitation in spring (March, April, and May), summer (June, July, and August), and autumn (September, October, and November).

Fig. 8. Relationships between daily net ecosystem carbon exchange (NEE), gross primary productivity (GPP), and ecosystem respiration (R_{ec}) and the average soil temperature (T_{soil}) and soil water content (SWC). Before the regression analysis, SWC was divided into two depth ranges: the near-surface soil (0 to 10 cm) and deeper soil (10 to 50 cm). However, NEE was only correlated with SWC at depths of 40 to 50 cm in the summer and 20 to 30 cm in the autumn based on the results of a collinearity test for the three seasons. T_{soil} was divided into a single range (0 to 50 cm) based on the results of a collinearity test for the three seasons: Spring (March, April, and May), summer (June, July, and August), autumn (September, October, and November).

Fig. 1.

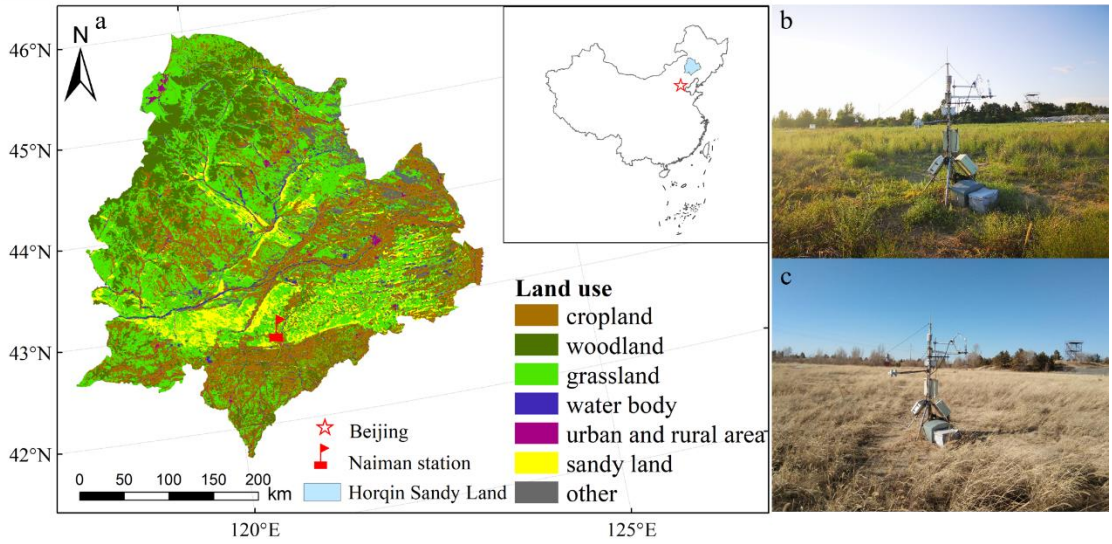

1013 **Fig. 2.**

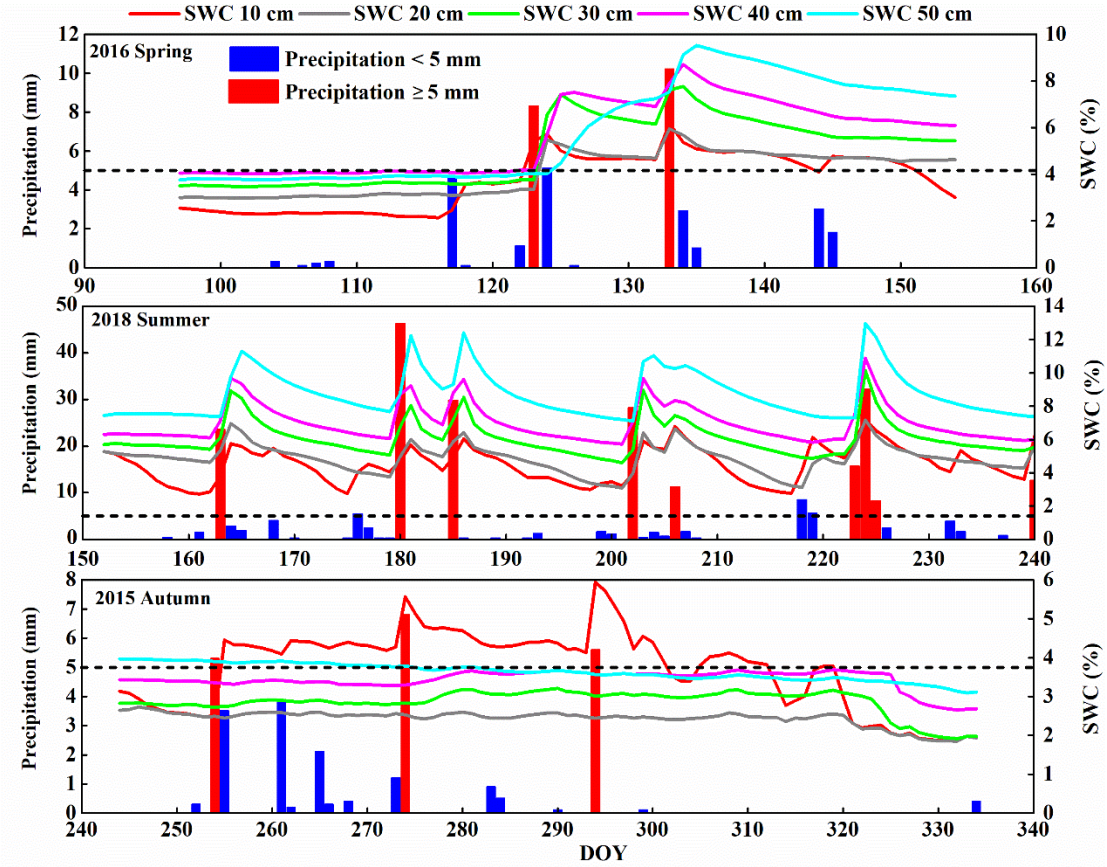

1014

1015 **Fig. 3.**

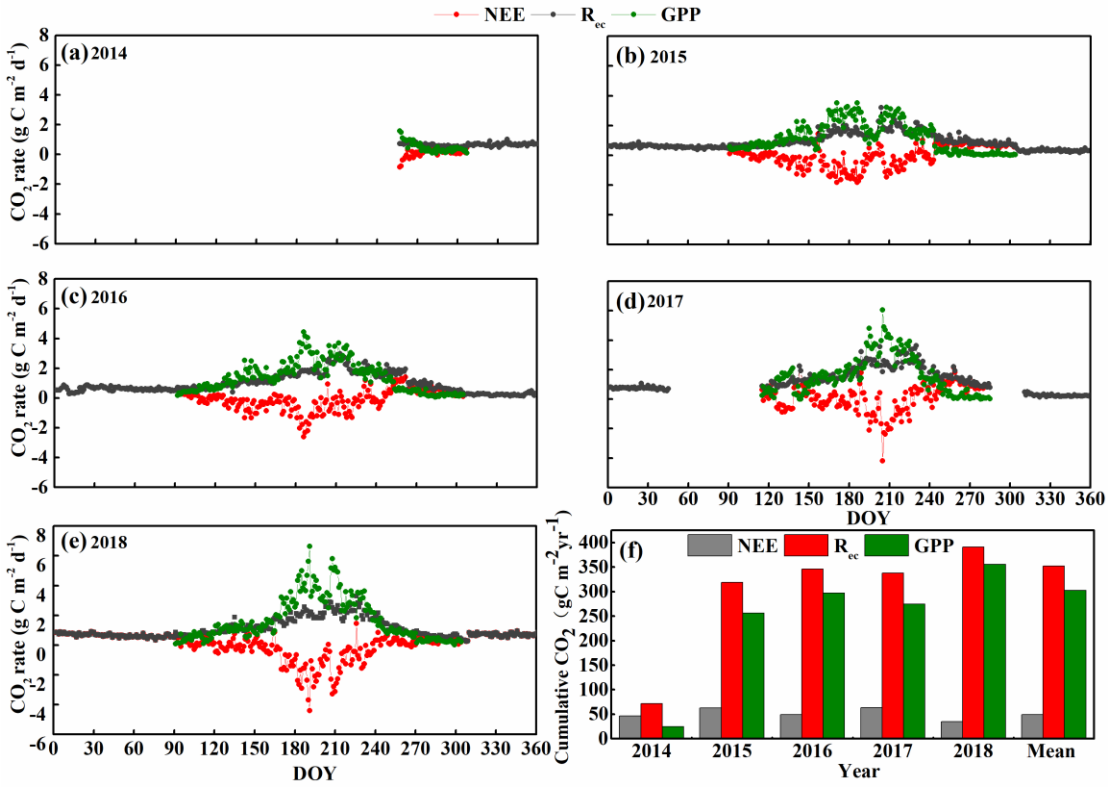

1016

1017 **Fig. 4.**

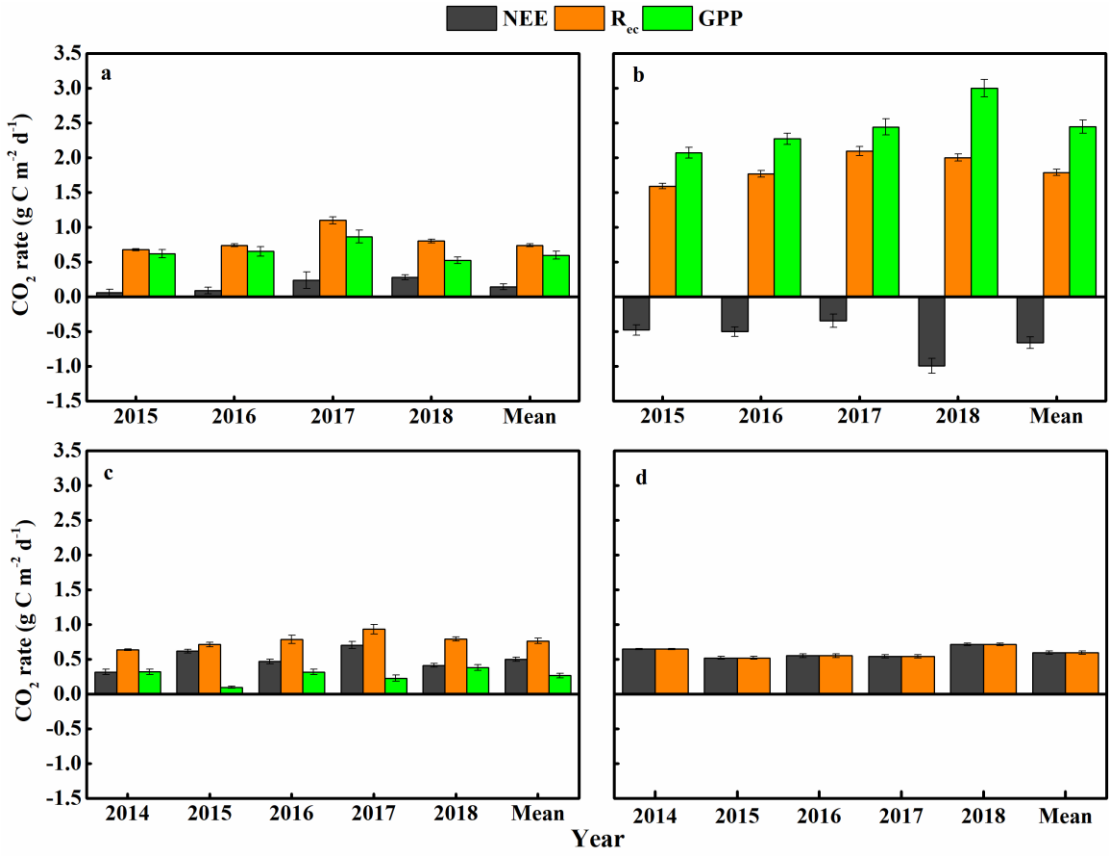

1018

1019 **Fig. 5.**

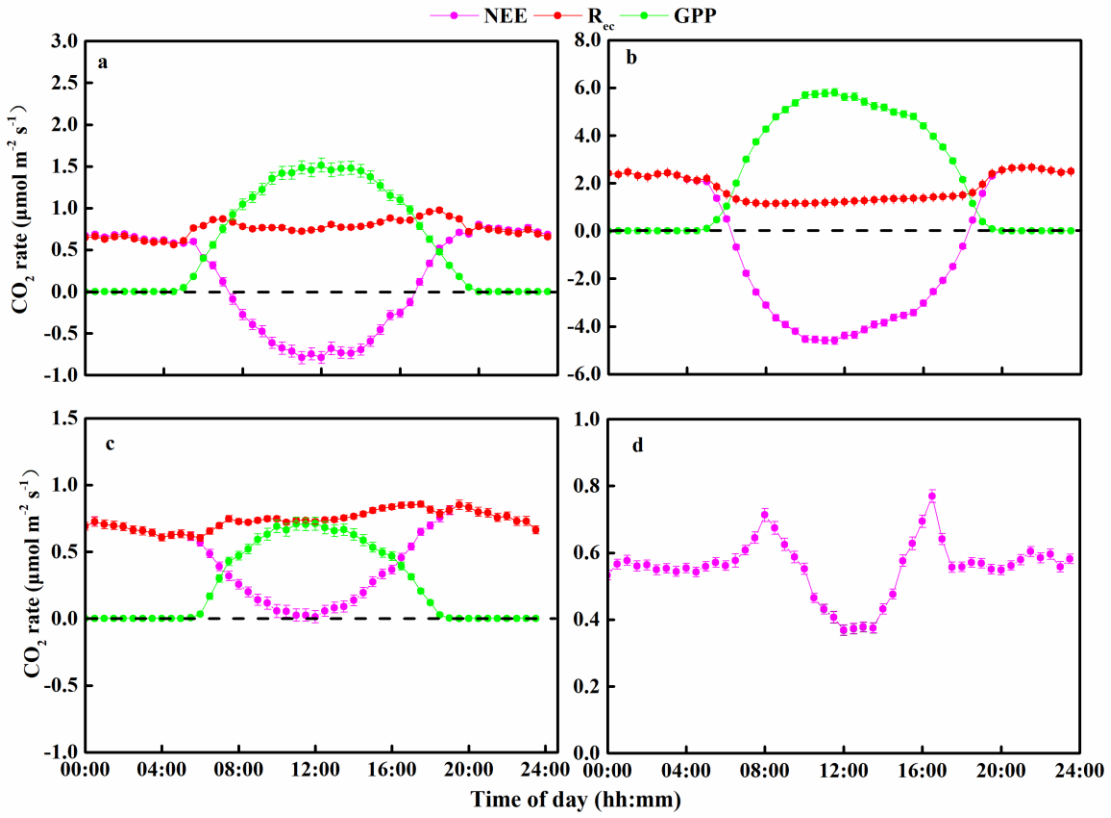

1020

1021 **Fig. 6**

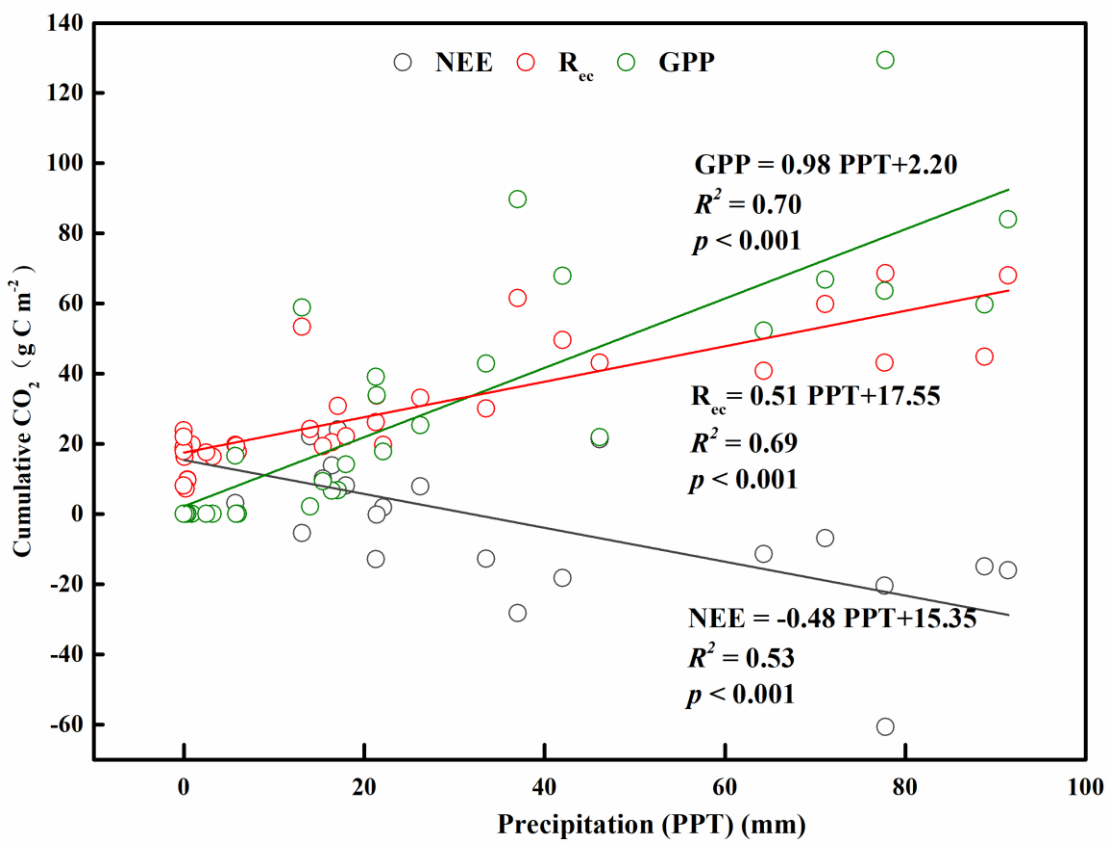

1022

1023

1024 **Fig. 7**

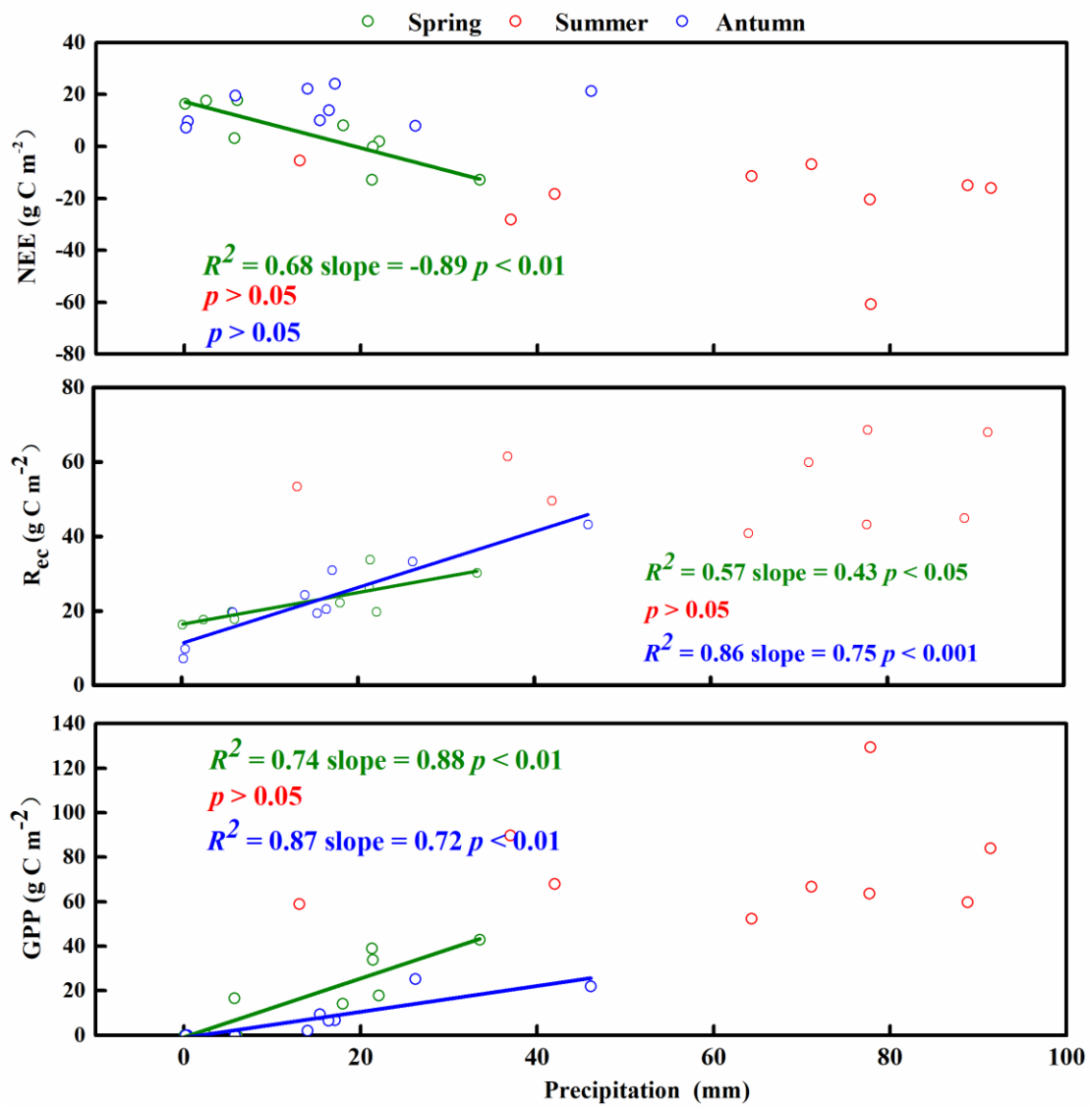

1025

1026

Fig. 8

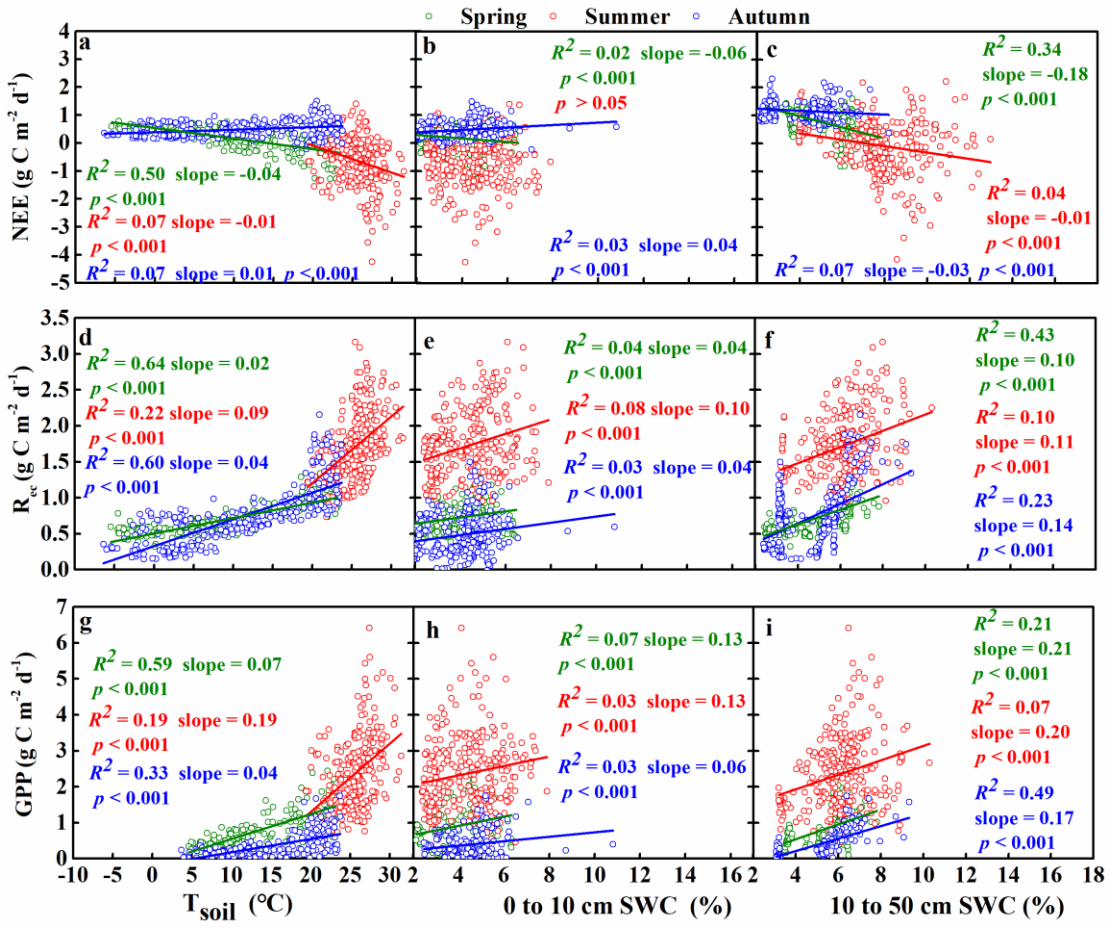

Table 1 Seasonal number of precipitation events for all years, grouped by size class and season, and the total precipitation.

Season	Year	Magnitude of precipitation event (mm)					Total Precipitation (mm)
		0-5	5-10	10-15	15-20	> 20	
Spring	2015	10	2	2	0	0	43.5
	2016	15	2	1	0	0	41.7
	2018	10	2	1	0	0	45.4
Summer	2015	22	7	3	0	0	132.8
	2016	39	5	3	2	1	172.4
	2018	26	4	2	1	5	258.0
Autumn	2015	13	3	0	0	0	31.5
	2016	12	2	1	0	1	62.7
	2018	9	1	2	0	0	47.4